

DEVELOPING MORE ACCURATE MODELS OF TORNADOS

Niall Bannigan^{1*}, Leigh Orf², Eric Savory¹

¹Mechanical & Materials Engineering, University of Western Ontario, London, Canada

²Space Science and Engineering Center, University of Wisconsin-Madison, Madison, USA

*nbanniga@uwo.ca

Abstract—Tornados are a major hazard and ever-present threat in many regions, with the potential to cause wide-scale loss of life and damage to infrastructure. Many researchers have attempted to develop tornado simulation techniques that amount to vortex generation with the goal of understanding the characteristics of tornado maintenance and intensity. Traditionally, these models comprise an analysis of wind-field data using Doppler radar collection, analytical tornado systems, laboratory experimental modelling, or the more recent numerical simulation techniques. These models, in application to wind engineering, focus on the tornado vortex without its parent storm and, as such, rely on artificial boundary conditions resulting in uniform, axisymmetric rotation about a vertical axis. The present work focused on developing superior tornado analysis techniques but first required generation of a method of tracking a tornado vortex centreline throughout its lifecycle, which corrects for the deficiencies in other vortex tracking methods when applied to tornados. The method identifies a clearly defined line for the vortex centre without need for extensive user-input. This method has been validated on the dataset of a tornado spawned from a supercell, in a meteorological numerical cloud model simulation at full-scale while being able to freely form and dissipate in a large, yet well-resolved, domain. Thus, quantitative assessment of a tornado wind-field may be anchored to an origin at the tornado centre that permits analysis of the discrepancy between the velocities of wind-fields generated by the previous models with those of a more physically realistic tornado. In future, analysis will be performed to understand how the in-flow at the simulation domain boundaries can be used to generate more accurate tornado models. This will provide the optimum ratio of tornado radius to the size of its domain and a set of detailed boundary conditions to apply to tornado simulations without the need to perform computationally expensive simulations. The work described above has provided findings that outline the extent to which current models of tornados underestimate their destructive potential and how they may be improved to provide superior engineering analysis.

Asymmetry; Boundary conditions; Tornado modelling; Velocity profiles; Vortex tracking

I. INTRODUCTION AND BACKGROUND

Tornados are rapidly rotating columns of air spawned by tall clouds such as thunderstorms that touch down on the earth's surface. Tornados above 2 on the Enhanced Fujita (EF) scale, a three second gust velocity greater than 55 m/s [1], develop from supercell thunderstorms [2] and while these violent tornados are also the least common, they cause the most damage and fatalities [3]. In the U.S.A, tornados are the cause of approximately 5000 fatalities since 1950 [4] and financial losses on the order of hundreds of billions of dollars [5]. Recent examples of such tragedies include Mayfield KY in December of 2021, Nashville TN in March of 2020, and several southern states in January of 2017 amounting to 93, 25, and 24 deaths and \$3.9, \$1.1, and \$1.2 billion in damage, respectively [5]. Improvements to forecasting and alarm systems during severe weather events has resulted in a dramatic reduction in the fatalities caused by tornados over the past several decades [6]. Further, the understanding of tornado behaviour has expanded through observational and numerical studies such that warning lead-times have increased [7] and building design codes have been updated to better withstand tornado wind-loading [8]. However, much work is still left to be done as the tornado false warning alarm rate is around 75% in the United States [9].

Tornados have been often modelled without a parent storm in the literature with focus on the key characteristics of the formation, translation, and structural wind-loading generation. Broadly, these attempts can be grouped into analytical models (e.g., [10], [11]), experimental models (such as the Ward-type [12], Purdue [13], and WindEEE dome [14] vortex chambers), and computer simulations using either Large Eddy Simulation (LES) (e.g., [15]) or Reynolds Averaged Navier-Stokes (RANS) (e.g., [16]) models. The ability to meaningfully analyze the data from any of the described tornado simulation methods depends on the data being processed such that their velocity and/or pressure-fields are comparable (e.g., [14], [16], [17]). To be able to quantitatively make such comparisons, one's results must be scaled in a commonly accepted manner. This often involves normalizing the circumferential profiles of tangential velocity, u_t , by the maximum $u_{t,max}$, and plotting against the radius from the tornado centre, r , normalized to r of $u_{t,max}$, R_t , (i.e. the vortex core) such as in Fig. 1 (e.g., [11], [14], [15], [16]). This technique provides a normalized tangential velocity profile

reminiscent of the Rankine vortex model [18]. Thus, the centre of the vortex is where this normalized velocity is zero and gives a meaningful datum for analyses. However, this position is often identified with minimal consideration of possible spatial fluctuation with time (e.g., [19]) and instead taken as the domain centreline (e.g., [13], [17], [20], [21], [22], [23]). For tornado models that are simplified, producing vortex flows with uniform conditions imposed at the domain boundaries, and focused not on the tornado dynamics found in meteorological research (e.g., [24]) itself but rather the wind-engineering applications (e.g., [15], [25], [26], [27], [28]) this is a reasonable approximation. Further, these are not unreasonable omissions for models that develop axisymmetric and fixed-location vortices (e.g., [15], [21], [29], [30]) or forced on a track (e.g., [16], [30], [31]) since the position is known by definition. It has also been shown that any meandering or asymmetry of a laboratory vortex may be neglected for very high swirl ratios, a measure of rotation strength, because the vortex is stable [32]. Finally, in [33] a low-pass filtering process (time constant of eight seconds) is employed to spatially and temporally average a wind-field. However, all of the aforementioned simplifications may be problematic if applied to a problem requiring detailed, instantaneous flow-field data such as when determining the peak wind-loading present on a building.

Tornado centre tracking methods have been reported in the literature, including the use of local maximum of the vertical component of vorticity then deploying a selection scheme based on mesh cell velocity derivatives [34], finding the location of minimal difference between velocity data and a simple Rankine vortex model [35], or using the location of zero tangential velocity, pressure gradient, and vorticity gradient [36]. There are other in-depth methods, described below, also available for implementation that are rarely used in conjunction with tornado vortex analyses (summarized in Table 1). In [37] the cosine of the angle between the velocity vector field, \mathbf{u} , and vorticity, ω , are determined and a vortex location is assigned for the region where this helicity value, H_n , is equal to $+/- 1$. Though this may not always occur, as noted in [37].

Another method in [38] introduces the λ_2 method that involves second largest eigenvalue of the symmetric tensor derived from the velocity gradient. This method provides reliable results for several flow-field applications but only identifies a region, rather than a single-point, to be the vortex not its centre.

A similar, but distinct, method is that of [39], which divides up three-dimensional (3D) mesh cells to find where slopes of the fluid flow streamlines is not definite within the cells and the velocity relative to the storm is zero. A filtering process is used

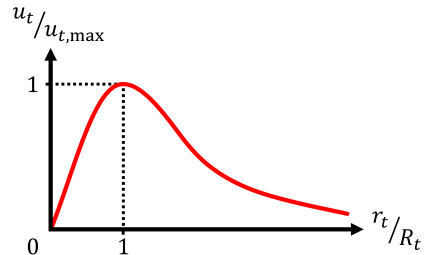


Figure 1. Example of a normalized tangential velocity plot

TABLE I. SUMMARY OF PREVIOUS VORTEX IDENTIFICATION METHODS

Method	Benefits	Drawbacks
Levy et al. (1990) [37]	<ul style="list-style-type: none"> • Single, simple analytical relation • Able to handle multiple vortices 	<ul style="list-style-type: none"> • Requires 3D data analysis • Criterion for detection is not necessarily true for vortices • Identifies a line of vorticity
Jeong and Hussain (1995) [38]	<ul style="list-style-type: none"> • Single, simple analytical relation • Able to handle multiple vortices 	<ul style="list-style-type: none"> • Cannot distinguish clustered vortices • Identifies a core region only
Sujudi and Haimes (1995) [39]	<ul style="list-style-type: none"> • Uses mathematical relation • Capable of identifying vortex as a point 	<ul style="list-style-type: none"> • Requires 3D data analysis
Jiang et al. (2002) [40]	<ul style="list-style-type: none"> • Simple criterion, easily implemented • No specific data grid type • Capable of identifying vortex as a point • Able to handle multiple vortices 	<ul style="list-style-type: none"> • Cannot distinguish clustered vortices without expensive iteration process
Wong and Yip (2009) [41]	<ul style="list-style-type: none"> • Able to handle skewed data grids • Identifies vortex as a point 	<ul style="list-style-type: none"> • Requires extensive user input to function at all

to check this and a reduced velocity, w , is checked for a pair of points of zero velocity indicating an intersection of a vortex centreline through the cell [39].

There is an algorithm in [40], which is able to highlight vortex regions using the grouping of vector orientations around said region. This method does not explicitly identify a vortex centre, but with several iterations could reduce the regions identified to a smaller point and thus taken as a centre.

Finally, the last method of interest, is that of [41], which is able to locate a centre of a vortex as a point, even if presented with off-skew horizontal flow-field data. The method finds the angle required to align velocity vectors to a spiral originated in a region of interest and then finding the area of most intersections extending from these vectors if they were rotated as described but it should be noted that this relies on *a priori* knowledge of the vortex centre [41].

Each of the methods mentioned have relevant applications to vortex modelling but fail to either precisely identify a centre point, operate in a computationally efficient manner, or operate without user-input/*a priori* understanding of the wind-field. The current work aims to meet all of these objectives and introduce a novel centre identification method to be able to relate the key characteristics of a tornado with its radius and track its motion through space and time even for complex, asymmetric, and realistically formed vortices.

II. METHODOLOGY

A. Tornado Data Source

The data in this paper are sourced from a large-scale supercell simulation performed on the National Centre for

Supercomputing Applications (NCSA) Blue Waters supercomputer utilizing a modified version of the Bryan Cloud Model, version 1 (CM1) model [42] [43]. This is a 3D, nonhydrostatic, fully compressive cloud model designed to study atmospheric phenomena such as thunderstorms. It is used in [24], as described above, to simulate some of the highest resolution thunderstorm simulations conducted to date and, in this work, to produce tornado spawning supercell thunderstorms. The simulation provided a tornado lifespan that is clearly defined for approximately 1300 single-second timesteps at 30-metre grid resolution forming naturally within a 3D environment, far from the domain boundaries (160-by-160-by-20-kilometres) and therefore unconstrained by artificial, uniform, forced boundary conditions. A constant velocity vector ($\mathbf{u}_b = 15.2\mathbf{i} + 10.5\mathbf{j}$ m/s) is subtracted from the dataset and a bounding box is placed around the tornado of 3.30-by-5.70-by-0.33-kilometres to approximately follow the tornado and provide a smaller area with which analysis may proceed. In this process, it became apparent that other methods of vortex centre identification would be insufficient in attempting to track the tornado for the detailed analysis desired, even within the limited-size domain captured.

B. Data Processing

It is important, when analyzing a tornado wind-field, to be able to specify a datum point about which all other discussion of the tornado characteristics may be situated. Thus, the novel method proposed in this work is detailed below to illustrate how the tornado data are unpacked and the centre location identified.

The data used in this work are in a Cartesian coordinate grid format, so for a tornado to be analyzed it is useful to recreate these data in cylindrical coordinates centred at the tornado centre. The tornado centre is defined herein as the region where the gradient of velocity, \mathbf{u} , is a local minimum and surrounded by a significant number of vectors of large ω in the horizontal plane based on [18] and [41]'s centre finding method. There are cases, both in nature and in supercell simulations, where multiple vortices of equal definition may appear together [44]. However, in the present study, only a single dominant vortex is apparent so analysis may proceed with only one vortex in mind. The method proposed begins with the wind-field sliced horizontally so that only a single 2D plane is considered at a time (Fig. 2a). The number of large ω identified is determined using

$$n_{scale} = \left\lceil \frac{\min[n_x, n_y]}{c} \right\rceil, \quad (1)$$

where n_{scale} is the scaling-factor rounded to the nearest integer, n_x is the number of grid points in x , n_y is the number of grid points in y , and c is a scaling parameter determined through trial-and-error (for this work, $c = 6$). Equation (1) ensures that, for a given dataset, the number of identified points are not so few that the search fails and not so many that erroneous locations are included in the analysis. In this work, $n_{scale} = 19$ (Fig. 2b). Following this selection, the spatial averages of the x and y positions of maximum ω , $\langle x_{curl} \rangle$ and $\langle y_{curl} \rangle$, and their standard deviations, $\sigma_{x,curl}$ and $\sigma_{y,curl}$, are computed. Using a desired number of standard deviations, n_s , as a cutoff, all points from the centre search that fall outside of the ellipse created by

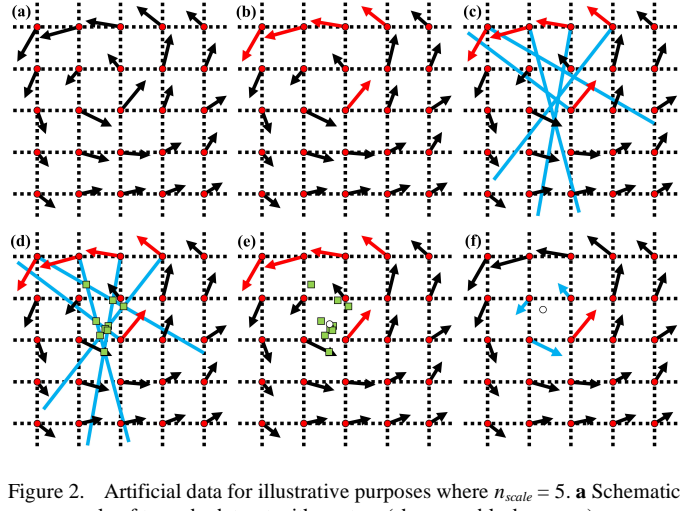


Figure 2. Artificial data for illustrative purposes where $n_{scale} = 5$. **a** Schematic example of tornado dataset with vectors (shown as black arrows) on an isotropic grid (shown as dashed lines); **b** 5 vectors (shown in red) selected based on n_{scale} ; **c** lines perpendicular to the selected vectors' orientation drawn (shown in blue); **d** identified intersections of each line drawn (shown as green squares); **e** location of average intersection identified (shown as white circle); **f** nearest vector identified (shown in red) and nearest vectors from identified vector that complete a loop (shown in blue) then used to interpolate for the location of zero-velocity (shown as white circle)

$$\frac{(x_{curl,i} - \langle x_{curl} \rangle)^2}{(\sigma_{x,curl})^2} + \frac{(y_{curl,i} - \langle y_{curl} \rangle)^2}{(\sigma_{y,curl})^2} \leq n_s, \quad (2)$$

are eliminated. This ellipse is centred on $[\langle x_{curl} \rangle, \langle y_{curl} \rangle]$ and has lengths $2n_s^{1/2} \sigma_{x,curl}$ and $2n_s^{1/2} \sigma_{y,curl}$. The points that remain are refined further using a technique derived from that in [41]. Their method is not applied directly here for its need of *a priori* information as mentioned previously. Here, lines extending perpendicularly from the locations of the identified vectors are drawn (Fig. 2c) and their intersections counted (Fig. 2d). Another round of averaging, as before, occurs here to eliminate erroneous intersections far from the tornado itself (Fig. 2e). Thus, the position of the final averaged point, once checked for errors, such as, no point has been found or it is very far from the location of minimum velocity, can either be replaced with the location of minimum pressure or, if valid, used in one final step to identify the true tornado centre. The point nearest to this average in the dataset is selected (Fig. 2f) and a grid of sidelengths c of data is taken from around it. This step is performed for the fact that a tornado centre is, as stated above, where the horizontal velocity should be zero. This position will likely be somewhere between the discrete grid points, so first the grid is checked for the lowest velocities (helpful if attempting to detect multiple vortices in close proximity to each other) and whichever is the lowest will be the centre of a new three-by-three grid. Of the remaining nine points, there are three vortex region cases to consider: rotation within one of the four quadrants; rotation within the east, west, north, or south quadrants; or rotation about the centre point (Fig. 3). A complete loop of a vortex is identified if the sum of the vector signs that form said loop is equal to zero in x and y directions, reminiscent of the technique described in [40], except that here

more types of vortex shapes may be identified. The number of successfully identified possible loops are stored and the sum of the tangential velocity magnitudes of each vector around each path compared between these loops so that the one with the smallest sum is determined to contain the vortex centre.

In a larger tornado or data of higher spatial resolution, this method may be implemented in an iterative fashion to reduce the size of the region being checked. If there is no successful path identified, then the search will eliminate the minimum velocity point chosen from future consideration and run the search within the c -by- c grid again as before, up to a total c number of times. If this still fails to yield a valid path, then the point used when an error occurs in the intersection averaging process is defaulted to as the tornado centre. Otherwise, the four corners of the loop found above are bi-linearly interpolated for the position that has $u_x = 0$ and $u_y = 0$. With this process complete, it is now trivial to perform analysis on any given tornado because its centre can be used as the origin of a cylindrical coordinate system and the vortex-relative radial, tangential, and vertical velocities may be utilized.

III. RESULTS AND DISCUSSION

The programmatic methods described above were applied to the simulated tornado-producing supercell dataset introduced previously. The fully tracked tornado centre is found in Fig. 4 for both the boundary-relative and the ground-relative tracking cases. The ground-relative tracking was created by simply multiplying \mathbf{u}_b by the time since the first timestep, t_s , and adding this distance to the location of each timestep's centre location, respectively. It was apparent that the path of the vortex could be defined to a high degree of accuracy even when near to the ground level, which is useful in being able to study wind-loading of infrastructure and buildings with respect to the vortex centre. For the sake of posterity, the algorithm searched the domain entirely from scratch upon each timestep. Though in practice, this would not be the case as the tornado cannot travel significantly each second. However, given that this was the worst-case scenario, the algorithm only failed to correctly interpolate for a tornado centre one time out of 1300 timesteps and all 11 horizontal layers. This equates to a failure rate of

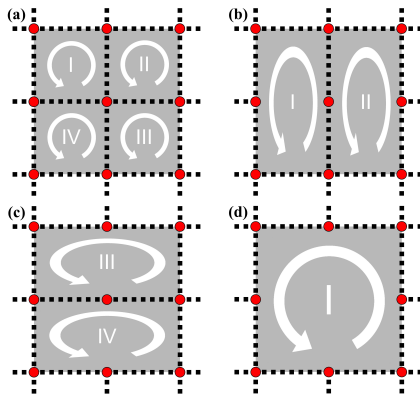


Figure 3. Schematic view of vortex region case checking where the red circles indicate the data points. Complete rotation loop in **a** one of the four quadrants; **b** left or right halves; **c** top or bottom halves; **d** the entire area

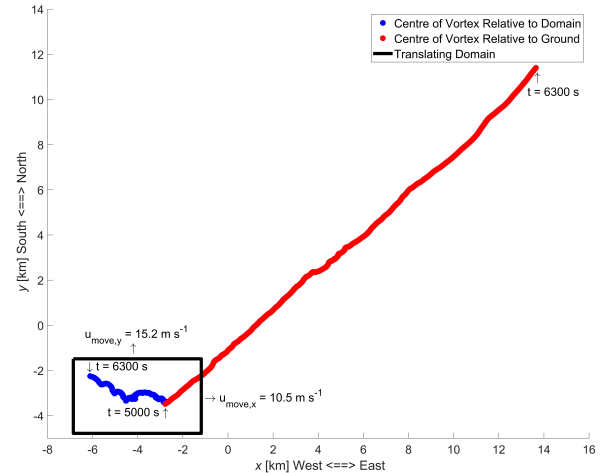


Figure 4. Plan view of the tornado following the centre at $z = 15$ m above ground level throughout the entire life cycle of the vortex relative to the dataset domain boundaries and relative to the ground

approximately 0.08% (when using $c = 6$), which is an acceptable rate since in such a case very few timesteps would need user-intervention to correct the error.

Using the full dataset domain of several arbitrary (but representative) timesteps and heights above ground level, the methods summarized in Table 1 are run alongside that which is proposed in this work to see how they perform relative to each other in execution efficiency (Table 2) and tracking accuracy (Fig. 5). It is clear from Table 2 that the fastest method is that of [40], averaging a solution time of just 0.52 milliseconds, followed closely by the method proposed in this work and by [37]'s method. Far slower are the methods proposed in [41], [39], and [40], in order of ascending solution time. The methods are all used without modification from the original authors' work.

Using [37]'s method, it was clear that the tornado in this dataset was one of the tornado's mentioned where H_n did not perfectly equal to $+/- 1$ and, strangely, it seemed that the tornado vortex was better defined where $H_n = 0$ (not shown in Fig. 5). However, the vortex was taken to be found where the angle between \mathbf{u} and ω was $< 15^\circ$. This appropriately outlines the

TABLE II. COMPARISON OF THE TIME TAKEN TO ANALYZE A GIVEN HORIZONTAL PLANE OF THE TORNADO

Analysis Method	Analysis Runtime per Horizontal Plane (10^{-3} s)	Analysis Runtime per Horizontal Plane (Normalized)
Levy et al. (1990) [37]	8.60	7.61
Jeong and Hussain (1995) [38]	0.52	0.46
Sujudi and Haimes (1995) [39]	8394.48	7428.74
Jiang et al. (2002) [40]	10786.20	9545.31
Wong and Yip (2009) [41]	202.55	179.25
Proposed Method	1.13	1.00

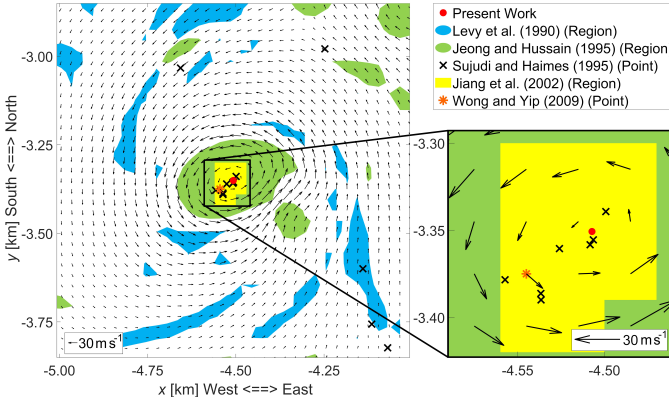


Figure 5. Comparison of the accuracy of various methods in tracking the vortex core centre on a representative wind-field data sample at $t_s = 5687$ s and $z = 165$ m above ground level

presence of the vortex (Fig. 5) but clearly does not provide a definite location of a tornado centre. It seemed that the method was now functioning as intended because, in this flow, u_z was often very small relative to the horizontal components of \mathbf{u} such that the two vectors were not as close to parallel as expected. The sense of the vortex direction was also not identified correctly as u_z flipped direction across the vortex unlike in [37], so this could not be relied upon to identify the direction of rotation. Additionally, to accommodate the use of the gradient it was necessary to expand beyond 2D solutions, increasing runtime.

The method in [38] was very effective at identifying the main vortex and even a smaller one (when present) but would need to be further processed in order to yield an exact centre location (Fig. 5).

[39]'s method required 3D analysis as the cell for the analysis had to have a height component, greatly increasing the computational demand. However, this method did very effectively identify possible centre locations (Fig. 5). It would require further processing in order to specify the true tornado centre.

The method of [40], although the slowest of all of the demonstrated methods, was able to capture the main vortex (Fig. 5). The reason that the region is selects is a regular geometric shape is that the area defined is just the region capturing the direction ranges as a binary result. Only the nearest neighbours to each given point of interest were analyzed and the data points were not interpolated to increase the accuracy, only in the interest of time was this omitted.

Using [41]'s method, a point was successfully identified and though it is within the vortex region it is not the true tornado centre (Fig. 5). To assist the program, a distance limiting the search from each vector had to be employed through trial-and-error to get the algorithm to produce meaningful results. This is yet another reason why this method would need much user-intervention as this method requires significant *a priori* knowledge. Combining this method with that of [35] would greatly reduce the amount of user-intervention necessary.

Finally, the method proposed in this paper was used and was able to clearly identify a tornado centre point (Fig. 5). The analysis ran without error and, qualitatively speaking, appears to

be the correct centre location in regard to the criteria laid out previously for a tornado centre. Though this only captures one vortex, it would be possible to expand this method to capturing multiple vortices if, for example, the curl locations used at the beginning of the analysis were weighted spatially and then grouped together to their nearest neighbours before the vortex search proceeds.

By taking the coordinate transformed data, it was possible to take the average tangential velocity around each circumference and identify the tornado core in Fig. 5 was approximately 260-metres in diameter. Comparing the proposed method with the other point searching methods, it is clear that [39]'s method was able to get as close as 5-metres to the true centre by as far away as 2-kilometres, representing a large margin of error. Alternatively, [41]'s method was able to get within only 45-metres of the true centre but this was after significant modifications and simplifications were made to format it to work with the dataset correctly.

IV. CONCLUSIONS

A methodology to identify the precise location of a tornado's centre has been developed. This method allows for superior centre tracking in comparison to previous work used in tornado research that assume the centre is in a fixed location, place the vortex *a priori*, or require user-intervention. This method finds a centre at each time step and horizontal slice of data. Previous vortex identification methods have been demonstrated to be deficient in comparison to the presently described method as they are only able to highlight the region of the vortex, find several centre positions requiring post-processing, or offer an approximate centre location.

In future work, the centre search program may be improved to better identify additional vortices even for cases where it is not clear which is stronger than the other. Additionally, the proposed method, having precisely identified the centre of the tornado, permits additional analyses to examine the velocity profiles within the vortex, simulate the damage potential relative to the distance from the tornado centre, and track a tornado path throughout its life cycle for both real and simulated vortices. This will also allow for work in which analysis of the wind-field around the tornado at typical boundary locations of laboratory or small-scale numerical simulations, acting as a complex, nonuniform boundary condition template.

ACKNOWLEDGMENT

The authors should like to thank the Natural Sciences & Engineering Research Council (NSERC) of Canada and the University of Western Ontario for their financial support.

REFERENCES

- [1] S. Potter, "Fine-Tuning Fujita: After 35 years, a new scale for rating tornadoes takes effect," *Weatherwise*, vol. 60, no. 2, pp. 64-71, 2007.
- [2] J. Grams, R. Thompson, D. Snively, J. Prentice, G. Hodges and L. Reames, "A climatology and comparison of parameters for significant tornado events in the United States," *Weather Forecast.*, vol. 27, pp. 106-123, 2012.

- [3] W. Lewellen, "Tornado vortex theory," in *The tornado: its structure, dynamics, predictions, and hazards*, vol. 79, C. Church, D. Burgess and R. Davies-Jones, Eds., Washington, Am. Geophys. Union, 1993, pp. 19-39.
- [4] National Centers for Environmental Information, "Storm Events Database," Natl. Oceanic Atmos. Adm., October 2021. [Online]. Available: <https://www.ncdc.noaa.gov/stormevents/>. [Accessed 2 February 2022].
- [5] National Centers for Environmental Information, "Billion-Dollar Weather and Climate Disasters," Natl. Oceanic Atmos. Adm., December 2021. [Online]. Available: <https://www.ncdc.noaa.gov/billions/events/US/1980-2021>. [Accessed 2 February 2022].
- [6] C. Doswell, A. Moller and H. Brooks, "Storm spotting and public awareness since the first tornado forecasts of 1948," *Weather Forecast*, vol. 14, no. 4, pp. 544-557, 1999.
- [7] H. Brooks and J. Correia, "Long-term performance metrics for national weather service tornado warnings," *Weather Forecast*, vol. 33, no. 6, pp. 1501-1511, 2018.
- [8] E. Agee and L. Taylor, "Historical analysis of U.S tornado fatalities (1808-2017): population, science, and technology," *Weather, Clim., Soc.*, vol. 11, no. 2, pp. 355-368, 2019.
- [9] J. Lim, B. Liu and M. Egnato, "Cry wolf effect? Evaluating the impact of false alarms on public responses to tornado alerts in the southeastern United States," *Weather, Clim., Soc.*, vol. 11, no. 3, pp. 549-563, 2019.
- [10] H. Kuo, "Axisymmetric flows in the boundary layer of a maintained vortex," *J. Atmos. Sci.*, vol. 28, pp. 20-41, 1971.
- [11] Y. Wen and A. Ang, "Tornado risk and wind effects on structures," in *Proceedings of the 4th international conference on wind effects on buildings and structures*, London, 1975.
- [12] N. Ward, "The exploration of certain features of tornado dynamics using a laboratory model," *J. Atmos. Sci.*, vol. 29, no. 6, pp. 1194-1204, 1972.
- [13] C. Church, J. Snow, G. Baker and E. Agee, "Characteristics of tornado-like vortices as a function of swirl ratio: a laboratory investigation," *J. Am. Meteorol. Soc.*, vol. 36, no. 9, pp. 1755-1776, 1979.
- [14] M. Refan and H. Hangan, "Characterization of tornado-like flow fields in a new model scale wind testing chamber," *J. Wind Eng. Ind. Aerodyn.*, vol. 151, pp. 107-121, 2016.
- [15] Z. Liu, C. Zhang and T. Ishihara, "Numerical study of the wind loads on a cooling tower by a stationary tornado-like vortex through LES," *J. Fluids Str.*, vol. 11, no. 3, pp. 549-563, 2018.
- [16] D. Natarajan, "Numerical simulation of tornado-like vortices," The University of Western Ontario, London, 2011.
- [17] C. Baker and M. Sterling, "Modelling wind fields and debris flight in tornadoes," *J. Wind Eng. Ind. Aerodyn.*, vol. 168, pp. 312-321, 2017.
- [18] W. Rankine, "Motions of Fluids - Hydrodynamics," in *Manual of Appl. Mech.*, London, Charles Griffin and Company, 1877, pp. 574-577.
- [19] Z. Tang, C. Feng, L. Wu, D. Zuo and D. James, "Characteristics of tornado-like vortices simulated in a large scale ward-type simulator," *Boundary-Layer Meteorol.*, vol. 166, no. 2, pp. 327-350, 2018.
- [20] R. Davies-Jones, "Can a descending rain curtain in a supercell instigate tornadogenesis barotropically?," *J. Atmos. Sci.*, vol. 65, no. 8, pp. 2469-2497, 2008.
- [21] A. Altalmas and A. El Damatty, "Finite element modelling of self-supported transmission lines under tornado loading," *Wind Str.*, vol. 18, no. 5, pp. 473-495, 2014.
- [22] J. Wang, S. Cao, W. Pang and J. Cao, "Experimental study on effects of ground roughness on flow characteristics of tornado-like vortices," *Boundary-Layer Meteorol.*, vol. 162, no. 2, pp. 319-339, 2017.
- [23] A. Razavi and P. Sarkar, "Laboratory study of topographic effects on the near-surface tornado flow field," *Boundary-Layer Meteorol.*, vol. 168, no. 2, pp. 189-212, 2018.
- [24] L. Orf, "A violently tornadic supercell thunderstorm simulation spanning a quarter-trillion grid volumes: computational challenges, I/O framework, and visualizations of tornadogenesis," *Atmos.*, vol. 10, no. 10, pp. 578-601, 2019.
- [25] Y. Wen, "Dynamic tornado wind loads on tall buildings," *J. Str. Division*, vol. 101, pp. 169-185, 1975.
- [26] E. Savory, G. Parke, M. Zeinoddini, N. Toy and P. Disney, "Modelling of tornado and microburst-induced wind loading and failure of a lattice transmission tower," *Eng. Str.*, vol. 23, no. 4, pp. 365-375, 2001.
- [27] A. Shehata, A. El Damatty and E. Savory, "Finite element modeling of transmission line under downburst wind loading," *Finite Elem. Anal. Des.*, vol. 42, no. 1, pp. 71-89, 2005.
- [28] M. Refan, H. Hangan, J. Wurman and K. Kosiba, "Doppler radar-derived wind field of five tornado events with application to engineering simulations," *Eng. Str.*, vol. 148, no. 1, pp. 509-521, 2017.
- [29] A. Hamada and A. El Damatty, "Behaviour of guyed transmission line structures under tornado wind loading," *Comput. Str.*, Vols. 11-12, pp. 986-1003, 2011.
- [30] T. Pecin, A. Almeida and J. Roehl, "Tornadic mechanical global actions on transmission towers," *J. Brazilian Soc. Mech. Sci. Eng.*, vol. 33, no. 2, pp. 131-138, 2011.
- [31] V. Beck and N. Dozek, "Reconstruction of near-surface tornado wind fields from forest damage," *J. Appl. Meteorol. Climatol.*, vol. 49, no. 7, pp. 1517-1537, 2010.
- [32] M. Refan, "Physical simulation of tornado-like vortices," The University of Western Ontario, London, 2014.
- [33] C. Wan and C. Chang, "Measurement of the velocity field in a simulated tornado-like vortex using a three-dimensional velocity probe," *J. Atmos. Sci.*, vol. 29, no. 1, pp. 116-126, 1972.
- [34] R. Strawn, D. Kenwright and J. Ahmad, "Computer visualization of vortex wake systems," *AIAA J.*, vol. 37, no. 4, pp. 511-512, 1999.
- [35] C. Potvin, "A variational method for detecting and characterizing convective vortices in Cartesian wind fields," *Mon Weather Rev.*, vol. 141, no. 9, pp. 3102-3115, 2013.
- [36] Y. Aboelkassem, G. Vatistas and N. Esmail, "Viscous dissipation of Rankine vortex profile in zero meridional flow," *Acta Mech. Sinica*, vol. 21, no. 6, pp. 550-556, 2005.
- [37] Y. Levy, D. Degani and A. Seginer, "Graphical visualization of vortical flows by means of helicity," *AIAA J.*, vol. 28, no. 8, pp. 1347-1352, 1990.
- [38] J. Jeong and F. Hussain, "On the identification of a vortex," *J. Fluid Mech.*, vol. 285, no. 1, pp. 69-94, 1995.
- [39] D. Sujudi and R. Haimes, "Identification of swirling flow in 3-D vector fields," in *Proceedings of the 12th computational fluid dynamics conference*, San Diego, 1995.
- [40] M. Jiang, R. Machiraju and D. Thompson, "A novel approach to vortex core region detection," in *Joint Eurographics-IEEE TCVG symposium on visualization*, 2002.
- [41] K. Wong and C. Yip, "Identifying centers of circulating and spiraling vector field patterns and its applications," *Ptnr. Recognit.*, vol. 42, no. 7, pp. 1371-1387, 2009.
- [42] G. Bryan and J. Fritsch, "A benchmark simulation for moist nonhydrostatic numerical models," *Mon. Weather Rev.*, vol. 130, no. 12, pp. 2917-2928, 2002.
- [43] G. Bryan, "CM1 Homepage," University Corporation for Atmospheric Research, 2008. [Online]. Available: <http://www2.mmm.ucar.edu/people/bryan/cm1/>. [Accessed 29 June 2020].
- [44] L. Orf, R. Wilhelmson and L. Wicker, "Visualization of a simulated long-track EF5 tornado embedded within a supercell thunderstorm," *Parallel Comput.*, vol. 55, no. 1, pp. 28-34, 2016.